Optica Applicata, Vol. XL, No. 4, 2010

Influence of Fourier spatial filtering on multimode fiber bandwidth

GRZEGORZ STEPNIAK, LUKASZ MAKSYMIUK, JERZY SIUZDAK*

Institute of Telecommunications, Warsaw University of Technology,
Nowowiejska 15/19, 00-665 Warszawa, Poland

*Corresponding author: siuzdak@tele.pw.edu.pl

The paper investigates the influence of the amplitude spatial filtering of the launched light beam on the baseband width of multimode (MM) fiber frequency response. The filter is located on the confocal plane of an 4*f* imager. The theory presented is verified by an experiment. It is shown that an increase of 3 dB baseband frequency of MM fiber is possible but at the expense of filtration losses.

Keywords: data transmission, multimode fiber, spatial filtering, bandwidth.

1. Introduction

An important part of local area networks (LANs) infrastructure is based on multimode (MM) fibers. This is particularly true for intra-building networks. Migration to novel transmission protocols, such as 10 Gbit/s Ethernet, increases network informational capacity and brings about unavoidable rise of bit rate. Faster data transmission over MM fibers may turn out to be difficult, especially for legacy fibers. This is due to the modal dispersion that limits baseband width of these fibers. Several methods of overcoming the problem of insufficient bandwidth have been proposed. They include manufacturing of novel MM fibers with profiles optimized for laser sources (such as OM3 fiber), adaptive electronic equalization of fiber frequency response [1], application of multilevel/multipoint modulation formats [2], appropriate light launching at the fiber input (such as offset launch) [3], and spatial light filtering [4, 5]. The last solution may be employed either at the fiber input [4] or its output [5]. The spatial filtering at the fiber output increases the modal noise level if a coherent source is used [6]. Therefore, in this paper we will concentrate on the spatial filtering of light at the fiber input and investigate its impact on the frequency response of the MM fiber. Our setup is much simpler than that used in [4]. The latter additionally required an adaptive feedback for the operation optimization. Contrary to [4] we are looking for spatial filters that increase the MM fiber baseband without any feedback. This paper

is divided into two main parts: the first contains the description of the setup proposed and presents some theoretical results. The second part treats about the experimental results obtained. Eventually, the results of our investigation are summarized.

2. Theory

The setup for the light spatial filtering is located at the fiber input, which is shown in Fig. 1. It is a typical confocal 4*f* setup [7]. The light source (usually laser) is located on the input focal plane of the two confocal lens setup. On the common focal plane, there is placed a spatial (amplitude) filter. In turn, the transmission MM fiber front end is located on the exit focal plane of the setup, as shown in Fig. 1.

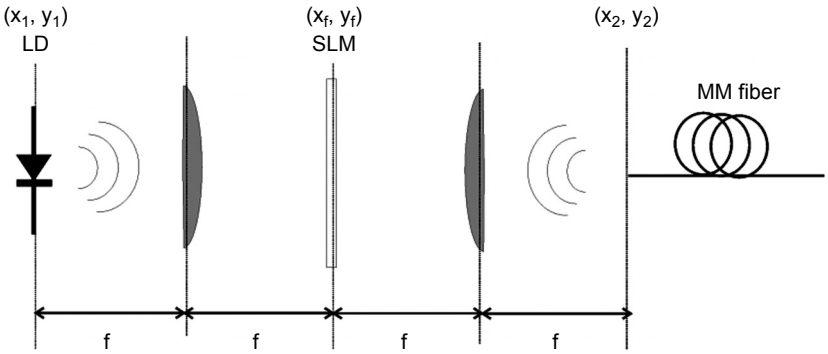

Fig. 1. Spatial filtering at the fiber input.

Let us denote by $A(x_1, y_1)$ the amplitude of the electromagnetic field originating from the light source. Then the field incident upon the spatial filter/modulator is given as two dimensional Fourier transform of $A(x_1, y_1)$ [7]

$$B(u, v) = \frac{1}{\lambda f} \int_{-\infty}^{+\infty} \int_{-\infty}^{+\infty} \mathrm{d}x_1 \, \mathrm{d}y_1 \, A(x_1, y_1) \exp\left[-j2\pi(ux_1 + vy_1)\right] \tag{1}$$

Here, λ is the wavelength, f is the focal length, and u and v are the so called spatial frequencies related to the coordinates x_f, y_f on the confocal plane by

$$u = \frac{x_f}{\lambda f}, \qquad v = \frac{y_f}{\lambda f} \tag{2}$$

Taking into account the presence of the spatial filter with the amplitude transfer function $T(x_f, y_f)$ and using (1) for the second lens, one may calculate the optical field distribution on the output focal plane, $C(x_2, y_2)$, *i.e.*, at the front end of the fiber. It is given by

$$C(x_2, y_2) = \frac{1}{\lambda f} \int_{-\infty}^{+\infty} \int_{-\infty}^{+\infty} \mathrm{d}x_f \, \mathrm{d}y_f \, B\left(\frac{x_f}{\lambda f}, \frac{y_f}{\lambda f}\right) T(x_f, y_f) \exp\left[-j2\pi\left(x_f \frac{x_2}{\lambda f} + y_f \frac{y_2}{\lambda f}\right)\right]$$

$$= \int_{-\infty}^{+\infty} \int_{-\infty}^{+\infty} \int_{-\infty}^{+\infty} \int_{-\infty}^{+\infty} \mathrm{d}x_1 \mathrm{d}y_1 \mathrm{d}u \, \mathrm{d}v \, A(x_1, y_1) T(u, v) \times$$

$$\times \exp\left\{-j2\pi\left[u(x_1 + x_2) + v(y_1 + y_2)\right]\right\} \tag{3}$$

If we assume the light source in the form of a point located at the origin of coordinates $A(x_1, y_1) = \delta(x_1, y_1)$ (the Dirac function), Eq. (3) reduces to

$$C(x_2, y_2) = \int_{-\infty}^{+\infty} \int_{-\infty}^{+\infty} \mathrm{d}u \, \mathrm{d}v \, T(u, v) \exp\left[-j\,2\pi(ux_2 + vy_2)\right] \tag{4}$$

It follows from Eqs. (3), (4) that changing the amplitude transfer function of the spatial filter $T(u, v)$ we are able to shape the field distribution at the front end of the MM fiber, and in this way also the order of modes excited in this fiber. Indeed, let us consider a LP_{mn} mode that may propagate in the MM fiber with the field distribution given by $\varphi_{mn}(x_2, y_2)$. Its amplitude, a_{mn}, will be given by

$$a_{mn} = \iint_S \mathrm{d}x_2 \mathrm{d}y_2 \, C(x_2, y_2) \varphi^*_{mn}(x_2, y_2) \tag{5}$$

Computing the mode amplitudes one may calculate the powers of the subsequent mode groups, P_k, $k = 1, 2\ldots$ Let us remember that the mode LP_{mn} belongs to the k-th mode group, when $k = 2n + m - 1$ [8]. We have for the k-th mode group

$$P_k = \sum_{2n + m - 1 = k} |a_{mn}|^2 \tag{6}$$

Having obtained the values of P_k we may calculate the MM fiber impulse $h(t)$ and frequency responses $H(f)$ based on the theory presented in [9]. They are the following

$$h(t) = \sum_k P_k \, \delta(t - \tau_k L) \tag{7}$$

$$H(f) = \sum_k P_k \exp(-j\,2\pi\,\tau_k L f) \tag{8}$$

Here, δ is again the Dirac function, τ_k is the unit group delay of the k-th mode group, and L is the fiber length.

3. Calculation results

For the numerical calculations of the mode fields and group delays in Eqs. (5), (7), (8) the finite element method presented in [10] was used. For a given index of refraction profile the mode field distributions $\varphi_{mn}(x_2, y_2)$ were calculated according to [10], which in turn enabled the calculation of mode group powers according to Eqs. (5), (6). This made it possible to calculate the fiber time and frequency responses (Eqs. (7) and (8)). The mode group unit delays were again calculated as in [10] but the profile dispersion was neglected as it requires precise information of the dopant concentration. The calculus was conducted for four types of spatial filters presented in Fig. 2: low pass (LPF), high pass (HPF), band pass (BPF), and band stop (BSF). For clarification, the LPF filter is a transparent hole with opaque surrounding. In Fig. 2, the black color stands for opacity and white for transparency.

The powers in mode groups for different spatial filters are shown in Figs. 3 and 4. The results are presented for a fiber with core diameter of 62.5 μm, NA = 0.275, profile parameter $g = 2.2$, $L = 0.5$ km, $\lambda = 665$ nm, and $f = 5$ cm. A point light source located

Fig. 2. Basic spatial filters (left to right): low-pass (LPF), high-pass (HPF), band-pass (BPF), band-stop (BSF).

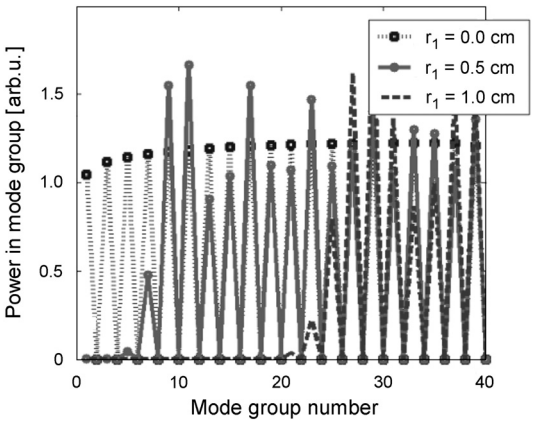

Fig. 3. Power in mode groups for HPF filter with radius r_1 ($r_1 = 0$ cm corresponds to the lackof filtration).

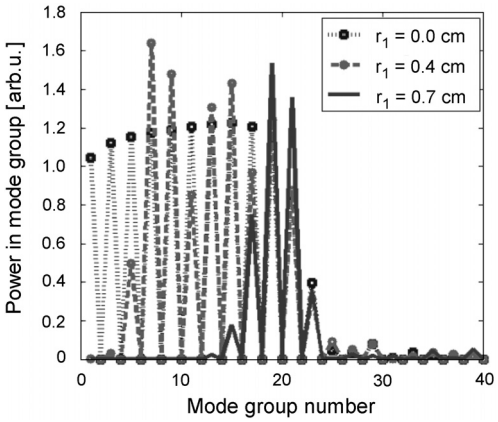

Fig. 4. Power in mode groups for BPF filter with outer radius r_2 = 1 cm and inner radius r_1 (r_1 = 0 cm corresponds to the low-pass filter).

at the origin of coordinates was assumed that resulted in the plane wave at the confocal plane. The wavelength was selected in accordance with the one used in the experimental setup. It follows from Figs. 3 and 4 that the filters used enable one to selectively excite the mode groups and in this way form the fiber frequency response. At the same time it is necessary to stress that the selectivity increase is obtained at the expense of the higher filtering losses.

Figures 5 and 6 present fiber frequency responses corresponding to different filters and mode excitations shown in Figs. 3 and 4. Eventually, Figs. 7–9 show the 3 dB baseband width values and corresponding losses (related to the spatial filtering) versus parameters of three different filters: low-pass, high-pass, and pass-band.

Additionally, in Figs. 10 and 11, we present numerical results of relative bandwidth improvement versus different filter radii for different alpha profile parameters. Relative improvement is understood as the times the bandwidth is increased with

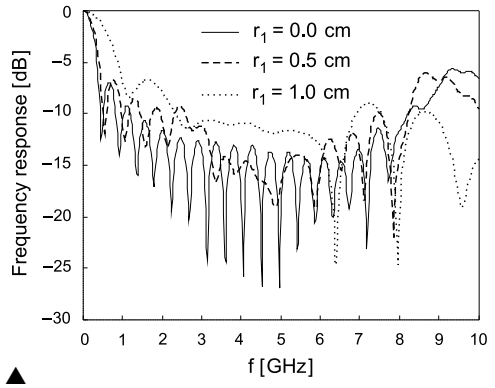

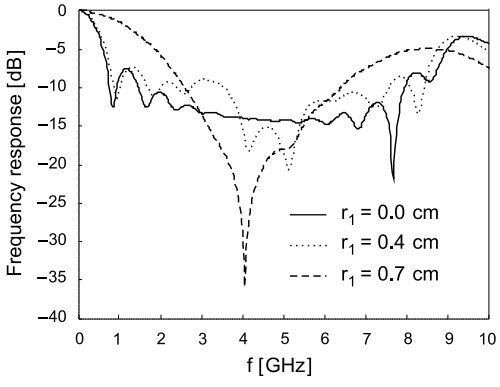

▲

Fig. 5. Frequency responses corresponding to the HPF filters and modal group excitation from Fig. 3.

Fig. 6. Frequency responses corresponding to the BPF filters and modal group excitation from Fig. 4.

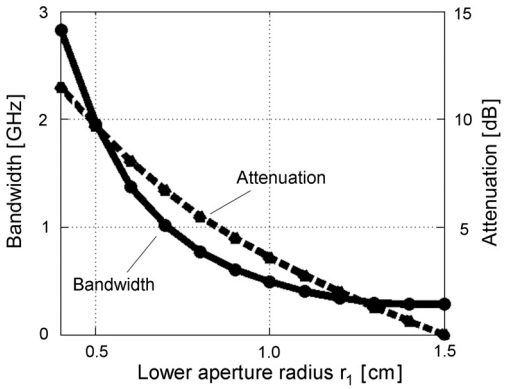

Fig. 7. Values of baseband width, and filtering losses for a LPF filter with different radii r_1.

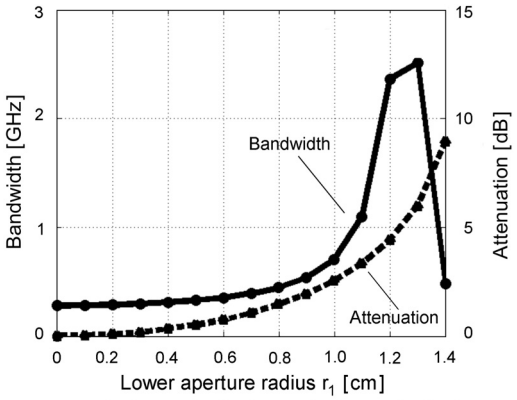

Fig. 8. Values of baseband width, and filtering losses for a HPF filter with different radii r_1.

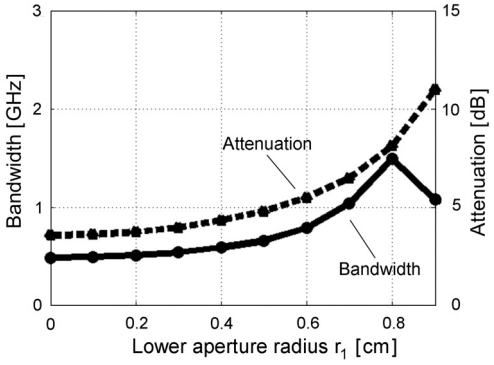

Fig. 9. Values of baseband width, and filtering losses for a BPF filter with $r_2 = 1$ cm and different radii r_1.

the use of the filter in comparison with the bandwidth of the fiber without a filter. As can be seen in Fig. 10, the highest improvement with the use of LPF is achieved for ideal alpha profile ($\alpha = 2$), whereas for BPF (see Fig. 11) better results are achieved for non-ideal profiles ($\alpha \neq 2$). Even though we notice a significant bandwidth improvement for BPF and $\alpha = 2$.

The results presented strongly indicate that the spatial filters may increase the baseband width of the MM fiber (the 3 dB frequency without filtering was 270 MHz

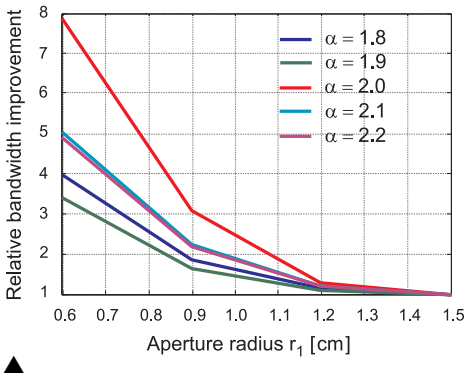

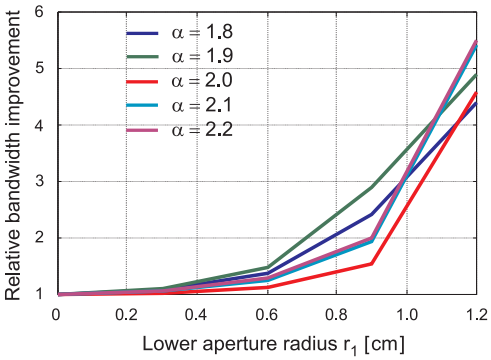

Fig. 10. Relative bandwidth improvement versus LPF filter radius.

Fig. 11. Relative bandwidth improvement versus BPF filter lower radius r_1, higher radius r_2 = 1, 3 cm.

in all the cases). The baseband width increase is achieved by eliminating/suppressing certain mode groups, which unavoidably reduces the total optical power launched into the MM fiber. If we assume a moderate value of this loss, 3 dB (optical), we are still able to increase the 3 dB baseband width 2–3 times (see results for HPF in Fig. 8).

4. Measurements

A block scheme of the measurement setup is shown in Fig. 12. The setup enables one to measure the MM fiber frequency response with the spatial filtering applied at its input. A generator with linearly swept frequency (coupled to the spectrum analyzer Rohde & Schwartz FSH6) drives a transmission laser (Hitachi HL 6504) that operates at λ = 660 nm.

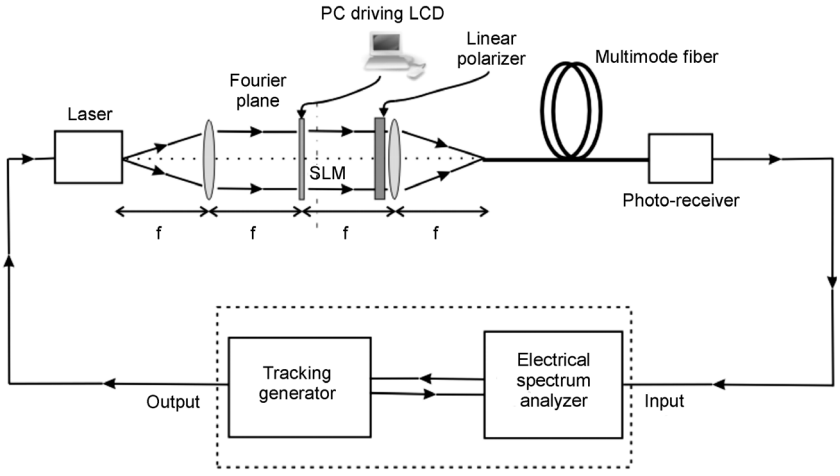

Fig. 12. Block scheme of the measurement setup.

The laser light after spatial filtering in 4*f* optical imager is focused at the front end of the fiber core (Corning Infinicor, 62.5 μm core and L = 500 m). At the confocal plane of the optical imager, there is a spatial light modulator (twisted nematic LCD, Holoeye LC 2002) with a single polarization filter added (polarization filter ahead of the spatial modulator was not necessary due to the linear polarization of the laser light). The polarization filter is necessary to obtain spatial amplitude filter (spatial light filtering). The LCD modulator is best suited for visible light and this forced the wavelength 660 nm to be used that is rather unusual for data transmission. The amplitude transfer function of the LCD modulator is controlled by a personal computer. After spatial filtering and propagation in the fiber the lightwave is detected by a Si photodetector (Hamamatsu S5973-01). After the OE conversion the electrical signal is fed to the spectrum analyzer measuring the frequency response of the entire system. The generator-spectrum analyzer set permitted the obtained frequency responses to be corrected for the non-uniformity of the system electrical response. Thus, all the results presented in the sequel pertain only to the optical responses.

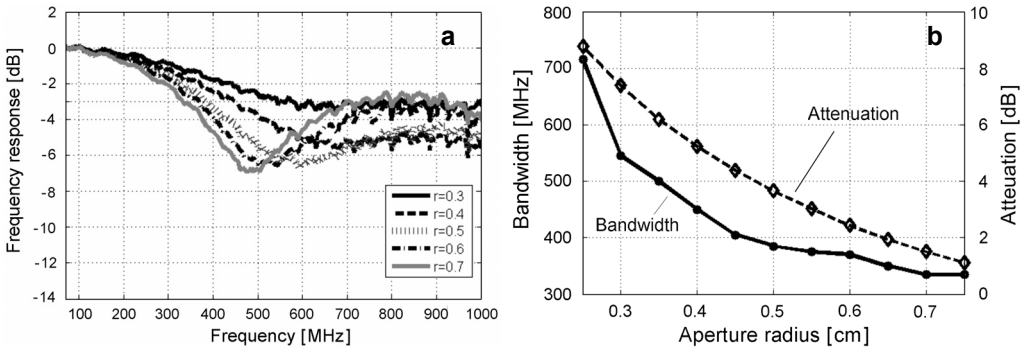

Fig. 13. Frequency response of the MM fiber (**a**) and baseband width, and filter losses (**b**) measured for LPF and different values of r_1.

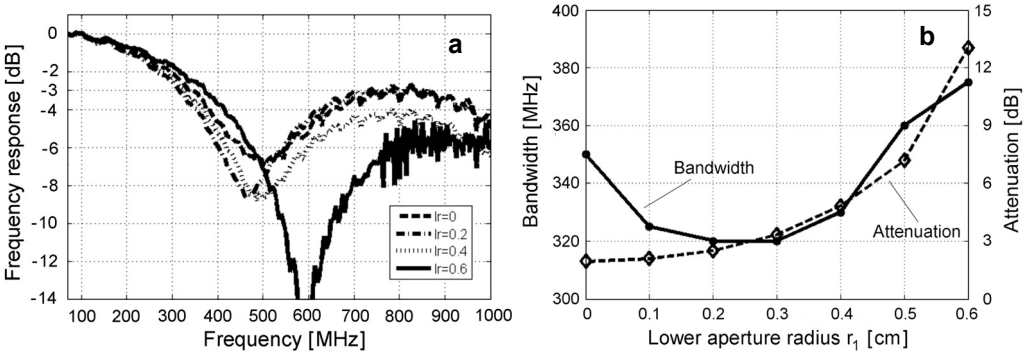

Fig. 14. Frequency response of the MM fiber (**a**) and baseband width, and filter losses (**b**) measured for BPF and different values of inner radius r_1 (outer radius was r_2 = 0.65 cm in all the cases).

In Figure 13, there are shown frequency responses for various low-pass filters (Fig. 13**a**) and corresponding values of baseband width and filtering losses (Fig. 13**b**). In Fig. 14, similar results are presented for band-pass filters, respectively. The 3 dB frequency (baseband width) without filter was 330 MHz.

The results presented in Figs. 13 and 14 are in qualitative agreement with the theory presented earlier. In particular, the greatest baseband width increase was obtained for low-pass filter, although at the expense of high losses. Also, the curves for the other filter behave similarly to the theory but the baseband width increase is much smaller than expected. The quantitative discrepancies may be explained by the fact that the actual lightwave at the confocal plane was not an ideal plane wave but rather an elliptical Gaussian beam. Moreover, the index profile of the real fiber was not measured and might have been different from the assumed one. Yet another reason might have been improper alignment and aberrations of the optical system as the required tolerances lay in micrometer range.

5. Conclusions

The paper presents the influence of the amplitude Fourier spatial filtering of the launched light beam on the baseband width of MM fiber frequency response. It was shown both theoretically and experimentally that this filtration may lead to an increase of a 3 dB baseband frequency. However, this increase is possible at the expense of filtration losses.

To implement these results in practice two issues should be addressed. First, the above calculations and experiments should be repeated for a representative set of the fibers with various index profiles. Second, as the $4f$ confocal set is not a practical one, the selected filters with the best properties should be realized in another way; most probably as a diaphragm integrated with the transmitter laser.

References

[1] XIA C, AJGAONKAR M., ROSENKRANZ W., *On the performance of the electrical equalization technique in MMF links for 10-gigabit ethernet*, Journal of Lightwave Technology **23**(6), 2005, pp. 2001–2011.

[2] LEE S.C.J, BREYER F., RANDEL S., GAUDINO R., BOSCO G., BLUSCHKE A., MATTHEWS M., RIETZSCH P., STEGLICH R., VAN DEN BOOM H.P.A., KOONEN A.M.J., *Discrete multitone modulation for maximizing transmission rate in step-index plastic optical fibers*, Journal of Lightwave Technology **27**(11), 2009, pp. 1503–1513.

[3] KOLESAR P.F., MAZZARESE D.J., *Understanding multimode bandwidth and differential mode delay measurements and their applications*, Proceedings of the 51st International Wire and Cable Symposium, 2002, pp. 453–460.

[4] SHEN X., KAHN J.M., HOROWITZ M.A., *Compensation for multimode fiber dispersion by adaptive optics*, Optics Letters **30**(22), 2005, pp. 2985–2987.

[5] PATEL K.M., POLLEY A., BALEMARTHY K., RALPH S.E., *Spatially resolved detection and equalization of modal dispersion limited multimode fiber links*, Journal of Lightwave Technology **24**(7), 2006, pp. 2629–2636.

[6] PETERMANN K., *Nonlinear distortions and noise in optical communication systems due to fiber connectors*, IEEE Journal of Quantum Electronics **16**(7), 1980, pp. 761–770.
[7] CHERUKULAPPURATH S., BOUDEBS G., MONTEIL A., *4f coherent imager system and its application to nonlinear optical measurements*, Journal of the Optical Society of America B **21**(2), 2004, pp. 273–279.
[8] OLSHANSKY R., KECK D.B., *Pulse broadening in graded-index optical fibers*, Applied Optics **15**(2), 1976, pp. 483–491.
[9] PEPELJUGOSKI P., GOLOWICH S.E., RITGER A.J., KOLESAR P., RISTESKI A., *Modeling and simulation of next-generation multimode fiber links*, Journal of Lightwave Technology **21**(5), 2003, pp. 1242–1255.
[10] LENAHAN T.A., *Calculation of modes in an optical fiber using the finite element method and EISPACK*, The Bell System Technical Journal **62**(9), 1983, pp. 2663–2694.

Received February 10, 2010
in revised form April 9, 2010